

A Novel Facial Cream Based on Skin-penetrable Fibrillar Collagen Microparticles

by RACHEL LUBART, PhD; INBAR YARIV, PhD; DROR FIXLER, PhD; and ANAT LIPOVSKY, PhD

Dr. Lubart is with the Chemistry Department and Physics of Bar Ilan University, Ramat Gan, Israel. Drs. Yariv and Fixler are with the Faculty of Engineering and the Institute of Nanotechnology and Advanced Materials at Bar Ilan University, Ramat Gan, Israel. Dr. Lipovsky is with Hava Zingboim Ltd., Ramat-Gan, Israel.

J Clin Aesthet Dermatol. 2022;15(5):59–64.

BACKGROUND: Collagen protein plays a notable role maintaining firm skin. Topical creams containing collagen fibers are widely available, but their usefulness is questionable due to limited skin penetration. When applied in a cream, collagen does not penetrate the skin leaving the skin structure unaffected. **OBJECTIVE:** We formulated micronized collagen in a cream base. Using human skin samples, we sought to investigate the ability of the micronized collagen cream to penetrate human skin. **METHODS:** Particle sizes of micronized marine collagen were evaluated using electron microscopy. Optical profilometry was conducted to evaluate skin topography and roughness. The antioxidant activity of the collagen was evaluated using the electron paramagnetic resonance technique by measuring the changes in free radical production. Collagen penetration depth in human skin samples was monitored using a non-invasive optical technique known as iterative multiplane optical property extraction, which works based on the detection of laser light phase changes following the presence of collagen particles in deep skin layers. **RESULTS:** According to the electron microscopy, collagen particles were found to be of various sizes, the smallest being about 120nm in diameter. Skin topography measurements revealed that the treated collagen cream increased skin smoothness of the samples. Our results derived from the iterative multiplane optical property extraction indicated that micronized collagen in a cream base penetrates both the stratum corneum and the deep epidermal layers toward the dermis. **CONCLUSION:** Our investigation suggests that the collagen in the studied cream formulation was able to penetrate the stratum corneum and deep epidermal layers in human skin samples. **KEY WORDS:** Fibrillar collagen, microparticles, skin penetration

Collagen is a fibrillar protein (polymer consisting of amino acids) that forms the conjunctive and connective tissues in the human body, especially the skin. This molecule is one of the most abundant in many living organisms due to its connective role in biological structures. It has been established that collagen fibers are damaged with the passage of time, losing thickness and strength, which has been strongly related with skin-aging phenomena. All proteins that have a structure based on three helix polypeptidic chains belong to the collagen family, with 26 types having been identified. It is not enough to have the right amount of collagen in the right place—it also has to be the collagen of the right type. The most abundant types of collagen in the skin are Types I and III; their fibrils being largely responsible for the skin's mechanical properties, such as strength, texture, and resilience.¹

Collagen has been used in skin creams for decades, with claims that it improves the structure of the skin. However, questions remain regarding the veracity of these claims. Collagen fibers are too large to penetrate

into the epidermis when applied to the surface of the skin. The effect of collagen is ascribed to its penetration.² Thus, it can be assumed that a collagen cream has no effect on skin. "Only collagen injections have some noticeable cosmetic effects, but since collagen injections are derived from the tissues of cows (often called bovine collagen), allergic reactions often occur following the injections, which has discouraged their use among many practitioners.

To overcome the challenge of poor penetration of the collagen fibers, formulation developers use partially hydrolyzed collagen (i.e., amino acids or peptides) that can penetrate the skin.³ Native collagen properties are different from those of hydrolyzed collagen. After denaturation, the triple-helix structure of native collagen changes to a random coil form due to dissociation of the hydrogen bonds when collagen undergoes hydrolysis.⁴ This process breaks the bonds in the polypeptide chain, resulting in a large number of peptides. These broken-down fragments cannot reassemble to build collagen in the skin layers.⁵ Peptides and amino acids do have

FUNDING: The study was sponsored by Hava Zingboim Ltd., Ramat-Gan, Israel.

DISCLOSURES: Drs. Lipovsky and Lubart are consultants with Hava Zingboim Ltd. The other authors report no conflicts of interest relevant to the content of this article.

CORRESPONDENCE: Rachel Lubart, PhD; Email: lubart@biu.ac.il

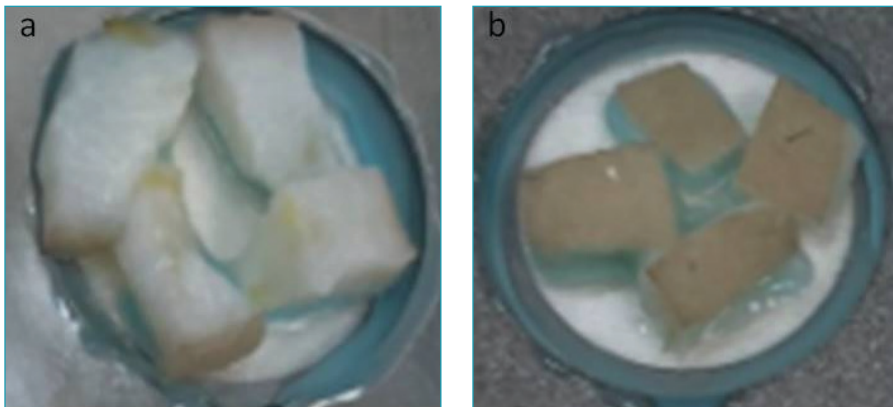


FIGURE 1. (A) Skin specimen preparation for ESEM; (B) Skin specimen preparation for profilometry

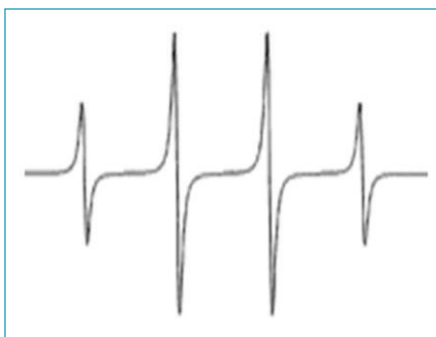


FIGURE 2. Typical DMPO-OH EPR spectrum

some beneficial biological functions, such as cell proliferation and a water-holding capacity, but they are different from those of collagen itself.⁶

In the present research, we prepared micronized marine collagen (m-collagen) fibers and inserted them into a cream. The micronized collagen in the cream was found to penetrate the stratum corneum (SC) barrier. We used collagen isolated from the *Molva molva* fish. Marine collagen is rich in type I and type III collagen, and its irritancy to the human skin is negligible.⁷ Particles size was measured by environmental scanning electron microscopy (ESEM) and dynamic light scattering (DLS) devices. Skin roughness following treatment with a cream containing m-collagen was evaluated by optical profilometry.

The antioxidant activity of collagen was evaluated using the electron paramagnetic resonance (EPR) technique by measuring the changes in free radical production in the presence or absence of microfibrillar collagen.

The depth of collagen penetration in human skin was monitored using a non-invasive optical technique called iterative multiplane optical property extraction (IMOPE).⁸ The technique uses a laser and camera for the detection of light

phase changes that can follow the presence of collagen particles in deep skin layers. The technique is based on light propagation through a diffuser substance, such as skin. Since the optical properties of light parameters are affected by the structure of the skin, they can monitor the presence of different particles within the skin layers. Optical profilometry was conducted for evaluating skin topography and roughness.

METHODS

Preparation of a cream with micronized collagen. The newly prepared m-collagen was inserted, at a 0.2% concentration, into a basic cream consisting of: aqua (water) without sodium hyaluronate, cetyl alcohol, silybum marianum ethyl ester, isoamyl laurate, hydrogenated soybean oil, steareth-21, cetearyl ethylhexanoate, castor isostearate succinate, theobroma cacao (cocoa) seed butter, hydroxyethyl urea, steareth-2, sodium pyrrolidone carboxylic acid, sodium lactate, fructose, glycine, niacinamide, urea, inositol, tocopherol, 1,2-hexanediol, dimethicone, caprylyl glycol, xanthan gum, polyacrylate crosspolymer-6, trisodium ethylenediamine disuccinate, *Magnolia officinalis* bark extract, ethylhexylglycerin, fragrance, and phenoxyethanol.

Determination of collagen fiber size.

The m-collagen was characterized using DLS and ESEM. During DLS, the hydrodynamic radius of the samples was measured with a particle analyzer (Zetasizer Nano-ZS; Malvern Panalytical, Malvern, United Kingdom). ESEM (FEI QUANTA-FEG 250; ThermoFisher Scientific, Waltham, Massachusetts) was conducted to assess the size of collagen and m-collagen

particles. Particle solution was dried on round coverslips (13 mm) and coated with iridium (Q150T ES; Quorum Technologies, Sacramento, California) prior to viewing.

Skin specimen processing and preparation for electron microscopy.

Fresh human skin samples were obtained (DA-TA BIOTECH; Rehovot, Israel) and were fixed in 10% buffered formalin and washed in sodium phosphate buffer at a pH of 7.2. Following overnight fixation, subcutaneous fat was partially reduced. Samples were cut, leaving safety margins of 1cm between each investigational site and the border of the tissue. For visualization, samples were glued to a round microscope coverslip (Figure 1A).

Samples were washed using phosphate-buffered saline at 37°C (02-023-1A; Biological Industries, Cromwell, Connecticut) three times (five minutes each) and primarily fixed with Karnovsky fixative buffer consisting of 2.5% (wt/vol) paraformaldehyde, 2.5% glutaraldehyde, and 0.1 M of cacodylate buffer for one hour at room temperature, then left overnight at 4°C.

The samples were dehydrated in a series of graded ethanol solutions (30%, 50%, 70%, and 95%, then three times at 100%), for 10 minutes each, then dried by vacuum critical point drying, which was performed using a Leica automatic EM CPD300 system (Leica, Wetzlar Germany) for 32 runs, with a cooling temperature of 7°C, a heating temperature of 40°C, stirrer speed set to 100%, and 100% advanced slow gas out.

Evaluation of skin topography. Skin topography and morphology were visualized by optical profilometry and ESEM, respectively. Optical profilometry was conducted for evaluating skin topography and roughness on wet skin after initial overnight fixation in 10% paraformaldehyde solution (Figure 1B) using a three-dimensional measuring laser microscope (Olympus LEXT OLS4100; Olympus Corp., Tokyo, Japan), allowing for a non-contact measuring of the microstructure surface. In order to do a comparative study of skin topography and roughness, the arithmetical mean roughness (S_a), arithmetical difference between the highest and the lowest points (S_z), and the root mean squared (RMS) roughness (S_q) were calculated. The (S_p) maximum peak height and (S_v) maximum valley depth were also measured.

Determination of antioxidative capability of collagen/m-collagen using EPR spectroscopy.

EPR is a sensitive technique for determining reactive oxygen species in certain conditions, such as the presence of hydroxyl radicals. In the present study, hydroxyl radicals were generated by performing a Fenton reaction with the following equation: $\text{Fe}^{2+} + \text{H}_2\text{O}_2 \rightarrow \text{Fe}^{3+} + \text{OH}^* + \text{OH}^-$.

Hydroxyl radicals have a short half-life (ns-ms), making them difficult to detect directly, there is a need to add a spin trap, which bounds the hydroxyl radicals, to yield a long-lived free radical, called a spin adduct, that can be detected by the EPR technique.⁹

We used 5,5-dimethyl-1-pyrroline-N-oxide (DMPO) to trap hydroxyl radicals to yield DMPO-OH, which has a quartet signal in the EPR spectrum. Figure 2 shows a typical EPR spectrum of DMPO-OH adduct, which is characterized by its 1:2:2:1 quartet of lines and hyperfine splitting constant a_N and $a_H = 14.9$. The area under the quartet signal is proportional to the amount of hydroxyl radicals.

When the Fenton reaction is performed in the presence of m-collagen or native collagen, there is a reduction in the quartet signal, which indicates its antioxidative activity.

In order to detect OH radicals, we used the sensitive technique X-band EPR spectroscopy coupled with spin trap DMPO. DMPO (38 mM; Sigma-Aldrich, St. Louis, Missouri) was purified with activated carbon (Thermo Fisher Scientific, Waltham, Massachusetts). The antioxidant activities of the compounds were determined by measuring the amount of hydroxyl radical produced via the Fenton reaction before and after the addition of collagen/m-collagen. The measured 100- μL aqueous suspensions mixture was comprised as follows: H_2O_2 (4400 μM , 10 μL) + FeSO_4 (500 μM , 10 μL) DMPO + DDW/collagen/m-collagen (10 μL) + MES buffer pH = 6 (65 μL) + DMPO (5 μL).

The mixture solution was introduced into a capillary micropipette (BRAND GMBH, Wertheim, Germany) and placed in a standard rectangular Bruker EPR cavity (ER 4119 HS) of the Bruker ELEXSYSE500cw X-band EPR spectrometer (Bruker, Billerica, Massachusetts). The room temperature spectra were acquired at a microwave frequency of 9.8 GHz, microwave power of 20 mW, and a sweep width of 100 G (centered at 3518 G) with a modulation amplitude of 1 G.

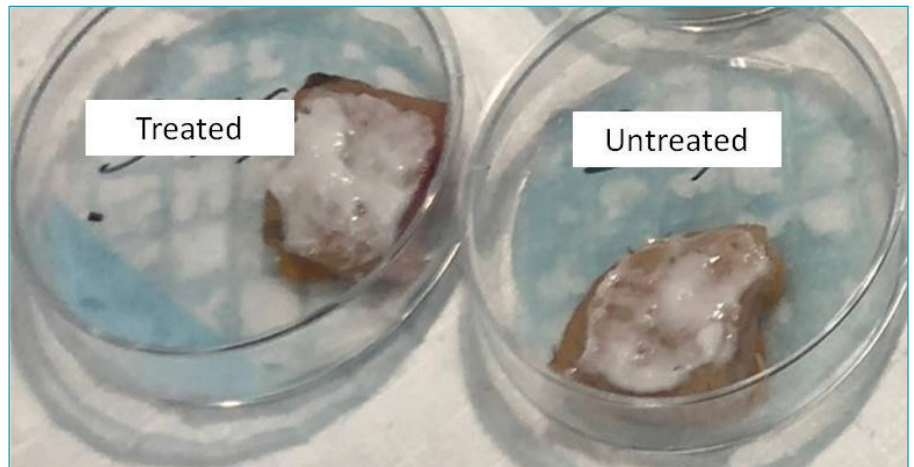


FIGURE 3. Skin samples following application of the treated and untreated collagen facial creams

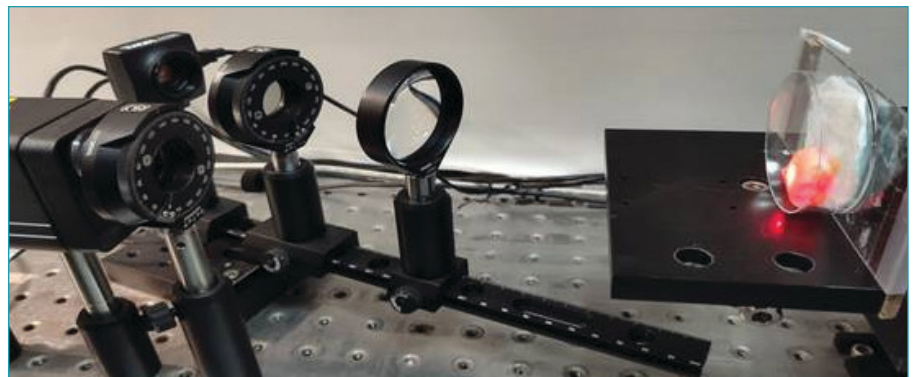


FIGURE 4. The experimental setup composed of a laser, polarizers for optical clearing purposes, a lens to focus the laser beam, and a camera for recording light-intensity images. The lens, polarizer, and camera assembly sits on a stage, which enables recording of images at different depths.

IMOPE measurements of skin penetration by the new collagen cream formulation.

The recently developed IMOPE technique is based on light propagation through a diffuser substance such as the skin. Since the optical properties of the light parameters are affected by the structure of the skin, they can monitor presence of different particles within the skin layers.

Skin sample preparation. Fresh human skin samples obtained (DA-TA BIOTECH; Rehovot, Israel) were examined macroscopically and microscopically to be intact without damage scars. Skin areas of 2cm² were treated in whole. Each cream sample (0.2 gr) was applied and spread gently by cotton swab. During treatment, skin samples were placed on top of moist fabric in 3.5-cm Petri dishes (Figure 3). The skin was kept moist with the applied cream for 3 h.

The evaluation of the penetration depth

of the collagen into the skin samples was conducted using the IMOPE technique.^{8,10–15} This technique extracts the reduced scattering coefficient based on the re-emitted light phase. The presence of particles within the tissue can affect the scattering value that is extracted. By assessing changes in the extracted scattering properties, IMOPE can sense the presence of particles at different depths in the tissue.

The IMOPE process starts with recording light-intensity images using an experimental setup. The intensity images are then used by an iterative algorithm¹⁶ for reconstructing the phase that had been lost once the images were captured. Having reconstructed the phase image, its distribution is calculated and compared to a theoretical model in order to extract the scattering properties of the sample.

IMOPE experimental setup. The experiments were conducted using the IMOPE experimental setup for recording light-intensity

TABLE 1. Topographical data

	SP (MM)	SV (MM)	SZ (MM)	SQ (MM)	SA (MM)
Test formulation	74.843	78.690	153.532	6.777	4.868
Control	70.171	88.716	158.886	8.653	6.201

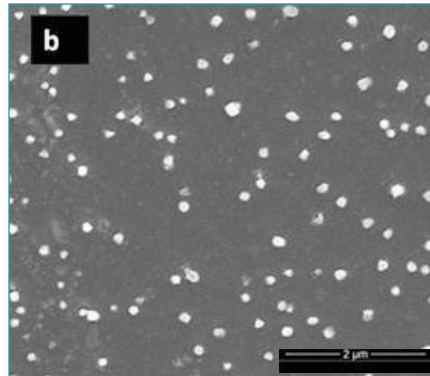
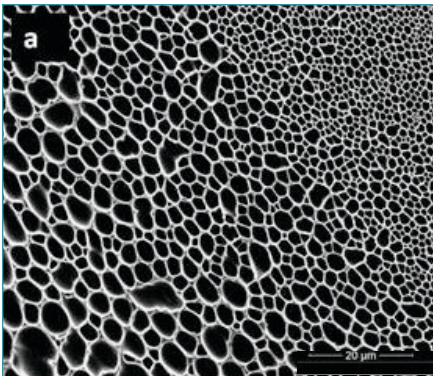


FIGURE 5. (A) Scanning electron microscopy image of the original collagen fibers; (B) Scanning electron microscopy image of the treated collagen fibers

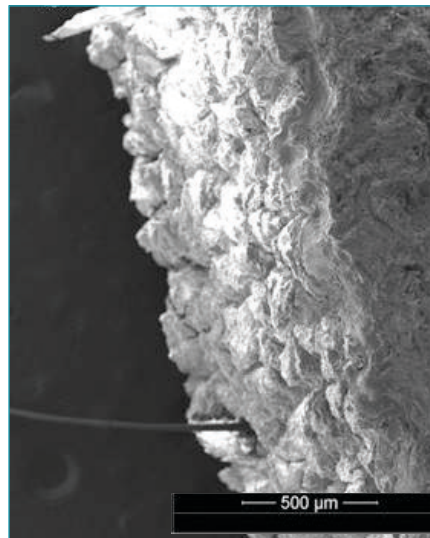
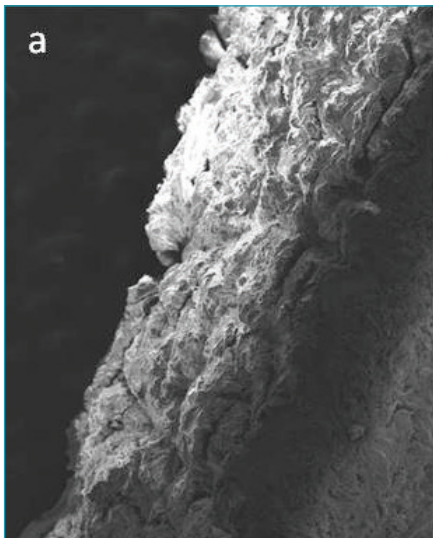


FIGURE 6. Cross-sections of the skin as taken by ESEM: (A) control and (B) treated cream

images at different locations along the z-axis, as presented in Figure 4. The experimental setup is composed of a laser with a wavelength of $\mu=633$ nm, which is preferable for biomedical applications. The other components within the setup were a lens, polarizers, and a CMOS camera (ThorLabs, Newton, New Jersey). The lens is used to focus the light beam, the polarizers for optical clearing purposes, and the CMOS camera for recording the light-intensity images. The skin samples were set on a three-axis micrometer stage (ThorLabs, Newton, New Jersey) for adjustments in the x, y and z directions. For each sample, three points were measured, the reflected phase was reconstructed, and its distribution, specifically

the RMS, was calculated using the IMOPE technique. The phase RMS was computed from a circular area with a radius size according to the tissue layer we were looking for.

For each tissue sample, we examined the computed RMS before applying the cream (0 h) and three hours after applying it (3 h). Since there is no real difference between the skin samples before applying the different creams, we calculated the average phase RMS at 0 h from all samples together.

To examine the penetration depth of the collagen, we conducted a depth-scanning analysis. During depth scanning, the phase RMS is computed along the z-axis. The phase RMS of each sample was computed using the

same algorithm parameters, a reconstruction thickness of 1.9 mm, and a distance between planes of 635 μ m. The reconstruction was completed along the z-axis, starting before the sample and advancing through the surface into the deeper layers.

Scattering properties of tissue layers. To analyze the IMOPE results, we first conducted a literature search for optical properties of human abdominal skin layers and their thicknesses.¹⁷ The skin tissue was divided into two layers, i.e., the SC (0.02 mm) and epidermis (0.1 mm). For each tissue layer, the phase RMS was calculated from a specific circular area in accordance with the tissue's scattering. With this method, in a single phase image in a specific scan, we can analyze different layers in different depths.

RESULTS

Collagen size. The purpose for reducing the collagen fibers size is to facilitate their delivery to deep human tissues. Once collagen microparticles cross the SC, they increase the skin's mechanical properties, such as strength, texture, and resilience.

In the present work, we used a new technique to produce a significant reduction in collagen fiber size. The reduced sizes were evaluated using DLS and electron microscopy techniques. The hydrodynamic size as measured by DLS was 368 ± 103 nm (polydispersity index [PDI], 0.959 ± 0.04). ESEM images showed (Figure 5) that the original mesh-shaped collagen fibers went through a micronization procedure, resulting in the formation of micronized collagen fibers with sizes of around 120 nm.

Mesh-structured collagen (Figure 5A) cannot enter the skin. Thus, when simply applied in a cream, collagen remains locked outside, without affecting the skin structure. However, our small treated collagen fibers, measuring around 120 nm (Figure 5B), can cross the SC and affect the inner skin structure.

Skin topography measurements following m-collagen face cream treatment

Profilometric data were obtained from analyzing skin samples treated with either the test formulation (base cream with m-collagen) or control (base cream with native collagen) at different magnifications ($\times 5$, $\times 10$, and $\times 20$). The results for the topographical data (at $\times 5$ magnification) are summarized in Table 1. The results show an improvement in skin topography in all parameters. Skin topography

was also visualized by ESEM imaging.

It can be observed in Figure 6B that, following the application of the treated cream, the SC layer seemed to be better connected to the stratum lucidum/stratum granulosum layers (Figure 6A).

Anti-oxidative activity of collagen and m-collagen. We observed an increase in the antioxidant activity of microfibrillar collagen (Figure 7C) compared to native collagen (Figure 7B). A 77% reduction in the intensity of OH radicals was observed following the addition of microfibrillar collagen, while a reduction of only 36% was observed with the native collagen.

Collagen skin permeation. It is difficult to detect changes in collagen amounts within the skin layers since skin is rich in collagen. Immunofluorescence-labeled antigen-based techniques failed to detect the penetration depth of collagen into the skin.

Recently, we succeeded in monitoring collagen penetration to the SC and epidermis skin layers using a new non-invasive optical technique called IMOP.⁸

Following computational analysis of the changes in the phase RMS as a result of application of a cream containing collagen on the skin samples, we could evaluate the presence (particle distribution) of treated (m-collagen) and untreated collagen in the SC and epidermis layers of human skin samples (Figure 8).

In Figure 8, only curves on the positive domain (y-axis > 0) monitor the existence of collagen particles in the depth of the human skin samples (SC and epidermis). It can be seen that treated collagen (m-collagen) exists in the SC (red line) and the epidermis (blue line). The amount of m-collagen in the epidermis was greater than that in the SC and increased in the deep epidermis layer. The native collagen (green and pink curves) remains on the skin surface. Three hours after application, the m-collagen reached the epidermis layer, whereas untreated collagen did not penetrate the skin at all.

CONCLUSION

The skin contains large amounts of collagen, whose fibers are responsible for the skin's mechanical characteristics, such as strength, texture, and resilience. One of the most important factors causing skin aging is a reduction in collagen in the dermal matrix.¹⁸

Native collagen (not hydrolyzed collagen)

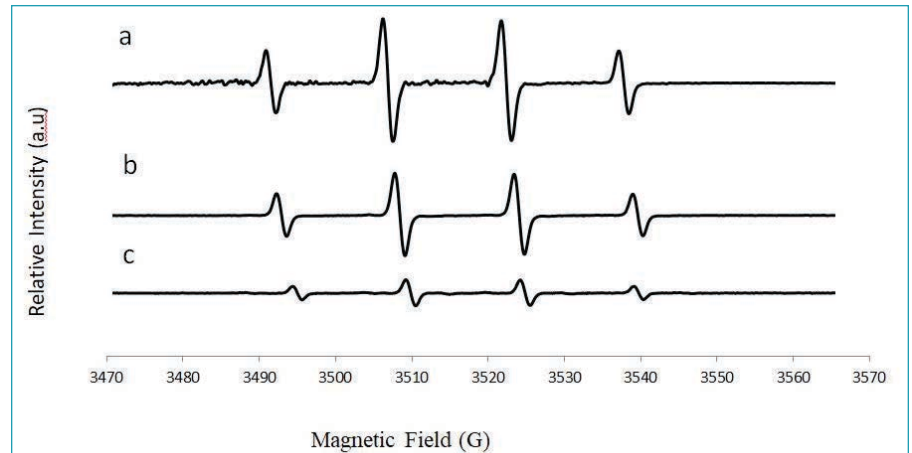


FIGURE 7. ROS formation: (A) Fenton, (B) collagen, and (C) microfibrillar collagen.

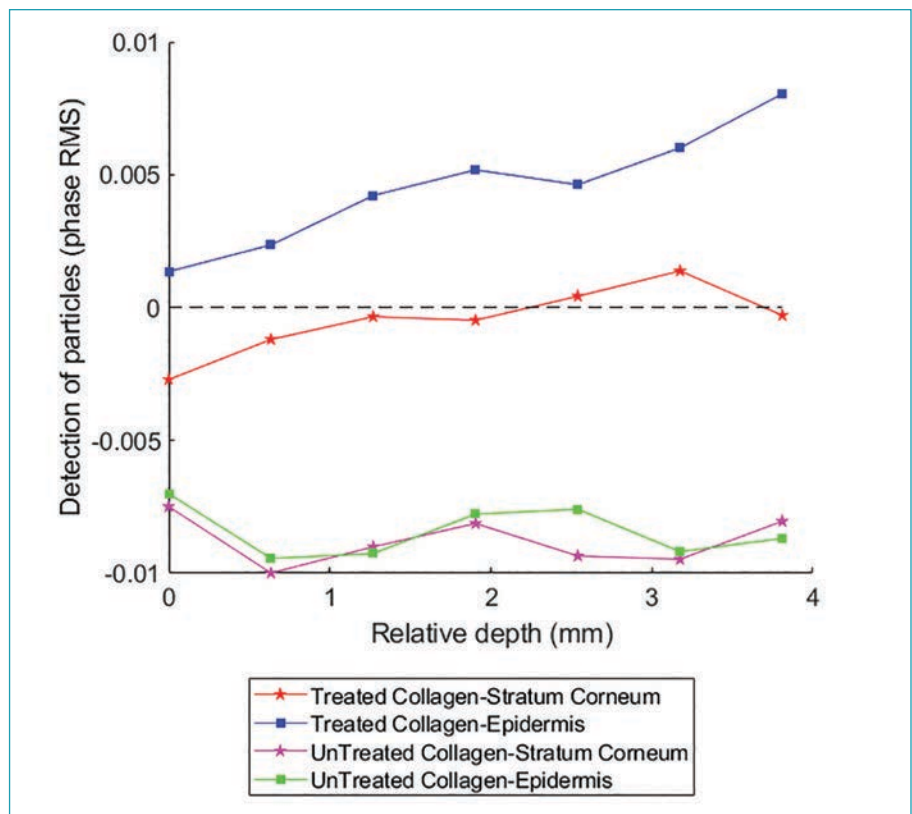


FIGURE 8. The phase RMS difference before and after applying the cream with treated/untreated collagen. For each skin sample, the change in the RMS, following the cream application, was computed for the SC (red and pink lines) and epidermis (blue and green lines).

cannot enter the skin barrier, so the available collagen creams in the market cannot replace the collagen lost to aging. The investigated facial collagen cream appeared to allow administration of fully functional collagen fibers into the deeper layers of the human skin samples. However, these collagen fibers are

smaller relative to those of native collagen, and can break down quicker in the skin. The IMOP technique is an excellent tool for identifying new added particles in the skin layers. However, it is impossible to exactly localize the particles within each specific skin layer.

ACKNOWLEDGMENTS

The authors would like to thank Dr. Ronit Lavi, Dr. Avi Jacob, and Mark Oksman for their assistance with EPR and microscopic measurements.

REFERENCES

1. Avila Rodríguez MI, Rodríguez Barroso LG, Sánchez ML. Collagen: A review on its sources and potential cosmetic applications. *J. Cosmet. Dermatol.* 2018; 17: 20–6.
2. Coapman S, Lichtin J, Adel S. Studies of the Penetration of Native Collagen, Collagen Alpha Chains, and Collagen Cyanogen Bromide Peptides Through Hairless Mouse Skin in vitro. *J Soc Cosmet Chem.* 1988; 39: 275–281
3. Aguirre-Cruz G, León-López A, Cruz-Gómez V, Jiménez-Alvarado R, Aguirre-Álvarez G. Collagen hydrolysates for skin protection: Oral administration and topical formulation. *Antioxidants.* 2020; 9: 181.
4. Gopinath A, Shanmugam G, Madhan B, Rao JR. Differential behavior of native and denatured collagen in the presence of alcoholic solvents: A gateway to instant structural analysis. *Int J Biol Macromol.* 2017;102: 1156–1165.
5. Shoulders MD, Raines RT. Collagen structure and stability. *Annu Rev Biochem.* 2009;78: 929–958.
6. León-López A, Morales-Peñaloza A, Martínez-Juárez VM, Vargas-Torres A, Zeugolis DI, Aguirre-Álvarez G. Hydrolyzed collagen-sources and applications. *Molecules.* 2019; 24: 4031.
7. Alves AL, Marques ALP, Martins E, Silva TH, Reis RL. Cosmetic potential of Marine fish skin collagen. *Cosmetics* 2017; 4: 39.
8. Yariv I, Rahamim G, Shlisselberg E, et al. Detecting nanoparticles in tissue using an optical iterative technique. *Biomed Opt Express* 2014; 5: 3871.
9. Buettner GR. Spin Trapping: ESR parameters of spin adducts 1474 1528V. *Free Radic Biol Med* 1987; 3: 259–303.
10. Yariv I, Kapp-Barnea Y, Genzel E, Duadi H, Fixler D. Detecting concentrations of milk components by an iterative optical technique. *J Biophotonics* 2015; 8: 979–84.
11. Yariv I, Haddad M, Duadi H, Motiei M, Fixler D. New optical sensing technique of tissue viability and blood flow based on nanophotonic iterative multi-plane reflectance measurements. *Int J Nanomedicine* 2016; 11: 5237–44.
12. Yariv I, Duadi H, Fixler D. Optical method to extract the reduced scattering coefficient from tissue: theory and experiments. *Opt Lett* 2018; 43: 5299.
13. Yariv I, Duadi H, Chakraborty R, Fixler D. Algorithm for in vivo detection of tissue type from multiple scattering light phase images. *Biomed Opt Express* 2019; 10: 2909–17.
14. Yariv I, Duadi H, Fixler D. An optical method to detect tissue scattering: theory, experiments and biomedical applications. In: *Proceedings of the SPIE, Volume 10891*, id. 1089105 9 pp. 2019. 2019: 3.
15. Yariv I, Shapira C, Duadi H, Fixler D. Media Characterization under Scattering Conditions by Nanophotonics Iterative Multiplane Spectroscopy Measurements. *ACS Omega* 2019; 4: 14301–6.
16. Gerchberg RW, Saxton WO. Practical algorithm for the determination of phase from image and diffraction plane pictures. *Opt* 1972; 35: 237–46.
17. Bashkatov AN, Genina EA, Tuchin V V. Optical properties of skin, subcutaneous, and muscle tissues: A review. *J Innov Opt Health Sci* 2011; 4: 9–38.
18. Janiš R, Pata V, Egner P, Pavlačková J, Zapletalová A, Kejlová K. Comparison of metrological techniques for evaluation of the impact of a cosmetic product containing hyaluronic acid on the properties of skin surface. 2017 DOI:10.1116/1.4985696. **JCAD**